Partial Discharge Inception Characteristics of LN_2/Polypropylene Laminated Paper Composite Insulation System for High Temperature Superconducting Cables

N. Hayakawa, T. Kobayashi, M. Hazeyama
Department of Electrical Engineering and Computer Science
Nagoya University
Furo-cho, Chikusa-ku, Nagoya 464-8603, Japan

T. Takahashi
Central Research Institute of Electric Power Industry (CRIEPI)
Electric Power Engineering Research Laboratory
2-6-1 Nagasaka, Yokosuka 240-0196, Japan

K. Yasuda
AC Equipment Engineering Department, Super-GM
Umeda UN Bldg., 5-14-10 Nishitenma, Kita-ku, Osaka 530-0047, Japan

and H. Okubo
EcoTopia Science Institute
Nagoya University
Furo-cho, Chikusa-ku, Nagoya 464-8603, Japan

ABSTRACT

Partial discharge (PD) inception characteristics of liquid nitrogen (LN_2)/polypropylene (PP) laminated paper composite insulation system for high temperature superconducting (HTS) cables were investigated in terms of the volume effect and the V-t characteristics. The electrical and optical measurements of PD inception characteristics showed that initial PD could be generated between PP laminated paper layers, as well as in a butt gap. Using a parameter called statistically stressed liquid volume (SSLV) based on the discharge probability in both butt gaps and LN_2-filled thin layers between PP laminated papers, we could systematically analyze and evaluate the volume effect on PD inception stress (PDIE). Furthermore, experimental results revealed that n values of V-t characteristics at PD inception were as high as 80-110. On the other hand, the lower n values obtained at breakdown were interpreted by the intensified PD development in thermal bubbles generated after the PD inception.

Index Terms — **High temperature superconducting cable, partial discharge, butt gap, volume effect, V-t characteristics.**

1 INTRODUCTION

APPLICATION of superconducting power technology to electric power apparatus such as power cables could give rise to enhanced power supply efficiency and capacity, compactness and environmental compatibility. Recent advancements in research and development of high temperature superconducting (HTS) cables have been significant [1−3]. For example, a 100 m long 3-phase 66 kV/1 kA HTS cable has successfully been developed by Tokyo Electric Power Company (TEPCO), Sumitomo Electric Industries, Ltd. (SEI) and Central Research Institute of Electric Power Industry (CRIEPI) in 2002 [1].

In order to incorporate HTS cables into the next generation power systems, the electrical insulation performance of such HTS cables should be reliable. A liquid nitrogen (LN_2)/ polypropylene (PP) laminated paper composite in-

Manuscript received on 4 September 2003, in final form 6 May 2004.

sulation system is regarded as the most promising system for the cold dielectric type HTS cables [4]. However, the butt gaps between the layers of laminated paper are the weak points where partial discharge (PD) generation can lead to the reduction of electrical insulation performance and to final breakdown. Since the practical, long-distance HTS cables would have more weak points, the size or the volume effect on the PD inception characteristics must be taken into account. V-t characteristics are very important components of reliable insulation design. Although V-t characteristics for LN_2/PP laminated paper insulation systems have already been investigated at breakdown stresses [5−7], few studies have so far focused on V-t characteristics at PD inception as the precursor of breakdown, which can be more crucial to the understanding of the insulation deterioration mechanism.

The PD inception characteristics of LN_2/PP laminated paper insulation for HTS cables have been presented in earlier publications [8, 9]. In this paper, the PD inception characteristics of LN_2/PP laminated paper insulation are discussed in terms of the volume effect and the V-t characteristics both at the PD inception. Combined electrical and optical measurements of PD inception characteristics allowed for the development of a universal expression for the volume effect on the PD inception stress (PDIE). Furthermore, on the basis of the measured V-t characteristics at a PD inception, the difference in the lifetime indices n of the V-t characteristics taken at a PD inception and at a breakdown voltage are discussed with respect to PD inception and breakdown mechanisms.

2 EXPERIMENTAL SETUP

To investigate the volume effect on the PDIE of LN_2/PP laminated paper insulation, two types of electrode systems were used: parallel plane and coaxial electrodes.

2.1 PARALLEL PLANE ELECTRODES

Figure 1 shows the parallel plane electrode system. PP laminated papers with butt gaps were sandwiched between parallel plane electrodes. The butt gap was simulated as a circular shape with 5 mm diameter, and the thickness of a PP laminated paper was 0.125 mm. Upper and lower electrodes were made of aluminum, and the upper electrode was molded in epoxy resin to avoid edge

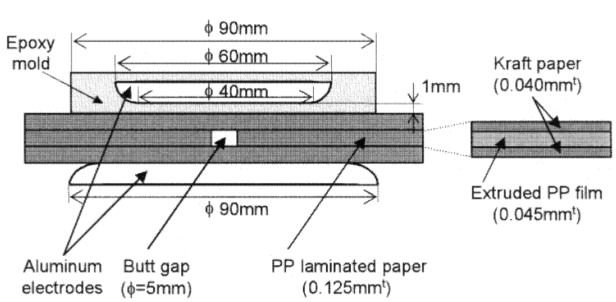

Figure 1. Parallel plane electrodes.

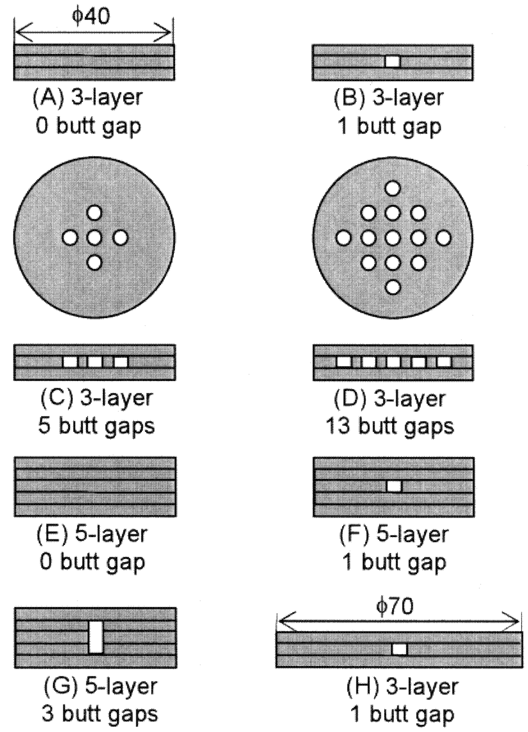

Figure 2. Arrangement of PP laminated paper layers and butt gaps for parallel plane electrodes.

discharges. Figure 2 shows various configurations of the specimens used.

2.2 COAXIAL ELECTRODES

Figure 3 shows the coaxial electrode system which has a larger insulation volume than the parallel plane electrodes. The sample was composed of three layers of PP laminated paper, each 0.125 mm thick, with the effective length of 100 mm. The inner electrode was 20 mm in diameter. The butt gap width was 1 mm.

2.3 EXPERIMENTAL SETUP

Figure 4 shows the experimental setup for the measurement of PD inception characteristics. The capacitor bushing was corona free up to 100 kV_{rms} in LN_2. The flat and

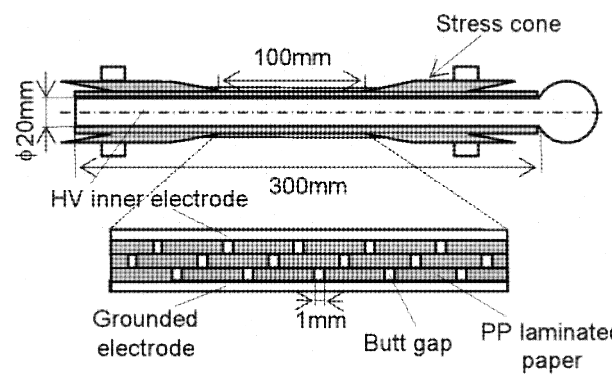

Figure 3. Insulation structure of coaxial electrodes.

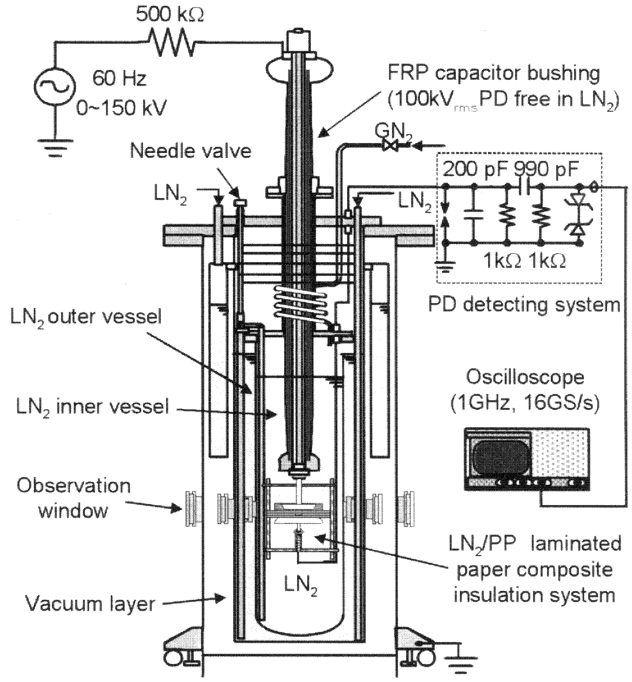

Figure 4. Experimental setup.

cylindrical specimens were immersed in LN_2 and stressed by ac 60 Hz high voltage. The PD inception voltage (PDIV) was measured for each specimen at least 20 times under a fixed condition. PDIV was then converted into PDIE, assuming the relative permittivity of PP laminated paper to be 2.2 and the relative permittivity of epoxy resin to be 4.7. The $PDIE_{50}$ corresponding to the 50% PD inception probability was evaluated using Weibull statistics. The sensitivity of the PD detection system was approximately 1.0 pC.

The V-t characteristics at PD inception were measured for parallel plane electrodes. The time to PD inception was measured for each specimen 10 times under a fixed applied electric field E_{ac} as the target stress. PD generation before reaching the target stress was included in the record of measurements. On the other hand, when PD was not generated for 1 hour after reaching the target stress, the measurement was stopped and also included in the record of measurements. The t_{50} corresponding to the 50% PD inception probability was evaluated using Weibull statistics. E_{ac} was taken as a parameter from 95% to 110% of the $PDIE_{50}$ for each specimen.

3 VOLUME EFFECT ON PD INCEPTION STRESS

3.1 PD INCEPTION STRESS

Figure 5 shows Weibull plots of PDIE for the specimen configurations A, B, C and D from Figure 2. The Weibull plots are used to determine $PDIE_{50}$ with a 50% cumulative probability for each specimen arrangement. Figure 6 shows $PDIE_{50}$ as a function of butt gap volume for the specimen configurations B, C, D, F, G and H. PDIE decreased with the increase in butt gap number under fixed specimen thickness and electrode size (see configurations B, C, D in Figure 2), which may suggest the effect of butt gap volume. However, PDIE also decreased with the increase of specimen thickness and electrode size under fixed butt gap number (see configurations B, F, H in Figure 2), where butt gap volume was constant. These results indicate that the $PDIE_{50}$ is affected not only by the butt gap volume, but also by some other factors as well.

	Sheet arrangement	Number of butt gaps	$PDIE_{50}$ [kV_{rms}/mm]	Confidence interval [kV_{rms}/mm]	Shape parameter m
○	A	0	41.17	41.14–41.20	18.4
△	B	1	38.37	38.35–38.39	14.7
□	C	5	33.93	33.88–33.97	13.7
◇	D	13	28.19	28.17–28.20	12.1

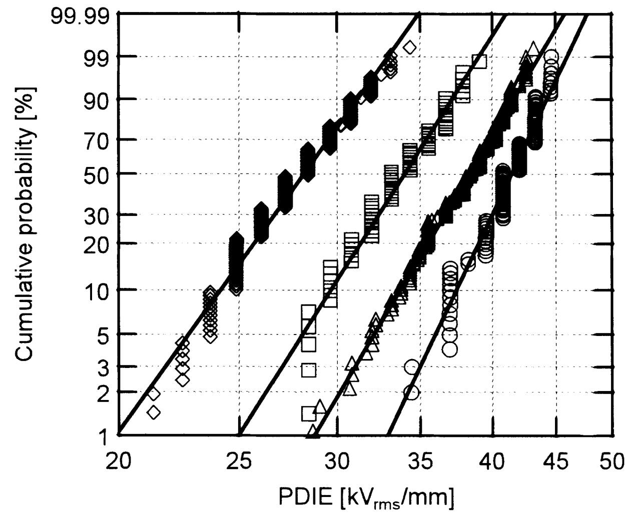

Figure 5. Weibull plots of PDIE for different specimen configurations (Flat specimens).

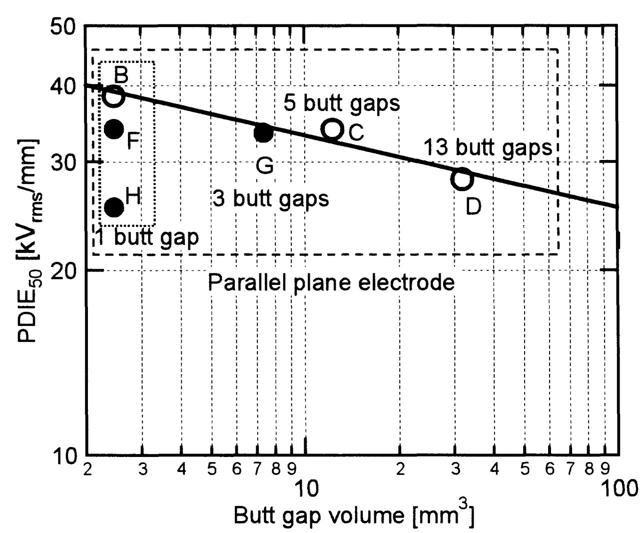

Figure 6. PDIE as a function of butt gap volume.

 1070-9878/05/$20.00 © 2005 IEEE

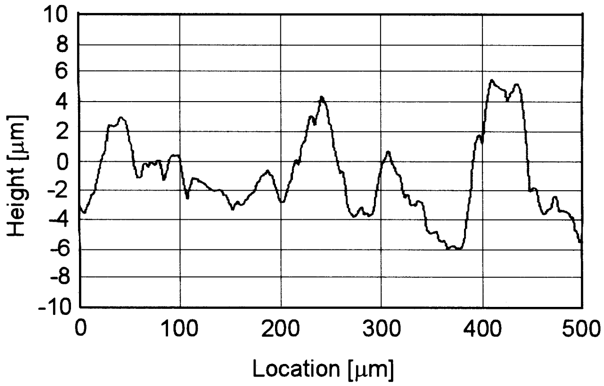

Figure 7. Typical surface roughness of PP laminated paper.

The above results suggest the presence of weak points for PD generation other than the butt gaps. We assumed that there are LN_2-filled areas between PP laminated layers associated with the surface roughness of PP laminated paper and that the total LN_2-filled volume is large enough to significantly contribute to PD generation. According to measurements of surface roughness of PP laminated paper (Figure 7), the average surface roughness is about 2 μm. This value was used as the LN_2-filled thin areas between the PP laminated paper layers.

In order to take into account the discharge probability based on the electric field distribution not only in the butt gaps, but also between PP laminated paper layers, the Statistically Stressed Liquid Volume (SSLV) parameter is introduced, according to equation (1) [10].

$$SSLV = \iint_V \int \left(\frac{E_i}{E_m} \right)^m dv \qquad (1)$$

where E_i is the electric field at a volume unit i, E_m is the maximum electric field, m is the Weibull shape parameter for PDIE, $(E_i/E_m)^m$ corresponds to the relative PD probability at the unit i.

Using equation (1), SSLV for butt gaps and the volume between insulation layers, calculated for different specimen configurations, are listed in Table 1. SSLV for the insulation volume between PP laminated paper layers was in most cases larger than that of the butt gaps. $PDIE_{50}$ values from Figure 6 were again plotted in Figure 8 as a function of SSLV. $PDIE_{50}$ decreased linearly in a log-log scale with increasing SSLV for different butt gap numbers, PP laminated paper layers and electrode size. This result can be regarded as the volume effect on $PDIE_{50}$ for parallel plane electrodes with different specimen configurations in Figure 2. In addition, the experimental result for the coaxial electrodes (Figure 3) is also plotted in Figure 8. $PDIE_{50}$ for all experimental arrangements could be fitted by a regression line expressed by the following equation:

$$PDIE_{50} = 90.1 \times SSLV^{-1/2.5} \quad [\mathrm{kV_{rms}/mm}] \qquad (2)$$

Table 1. SSLV and shape parameter for different specimen configurations.

Specimen configuration		$PDIE_{50}$ [kV_{rms}/mm]	Confidence interval [kV_{rms}/mm]	Shape parameter m	SSLV for butt gaps [mm^3]	SSLV between layers [mm^3]	Total SSLV [mm^3]
A	φ40, 3-layer 0 butt gap	41.17	41.14–41.19	18.4	0	7.54	7.54
B	3-layer 1 butt gap	38.37	38.35–38.39	14.7	0.9	7.42	8.32
C	3-layer 5 butt gaps	33.93	33.88–33.97	13.7	4.84	6.95	11.79
D	3-layer 13 butt gaps	28.19	28.17–28.20	12.1	14.08	6.01	20.09
E	5-layer 0 butt gap	32.25	32.19–32.30	13.9	0	12.57	12.57
F	5-layer 1 butt gap	34.03	33.98–34.07	17.8	1.02	12.37	13.39
G	5-layer 3 butt gaps	33.61	33.58–33.65	21.4	0.25	12.37	12.62
H	φ70, 3-layer 1 butt gap	25.31	25.22–25.41	12.2	1.08	22.89	23.97
	100, 3-layer	20.64	20.60–20.68	12.3	11.94	37.55	49.49

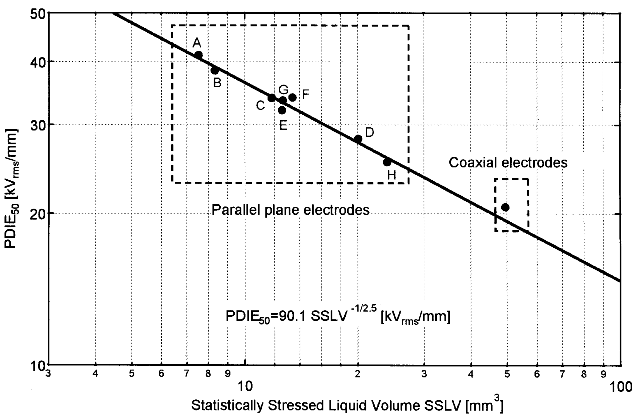

Figure 8. PDIE as a function of Statistically Stressed Liquid Volume (SSLV).

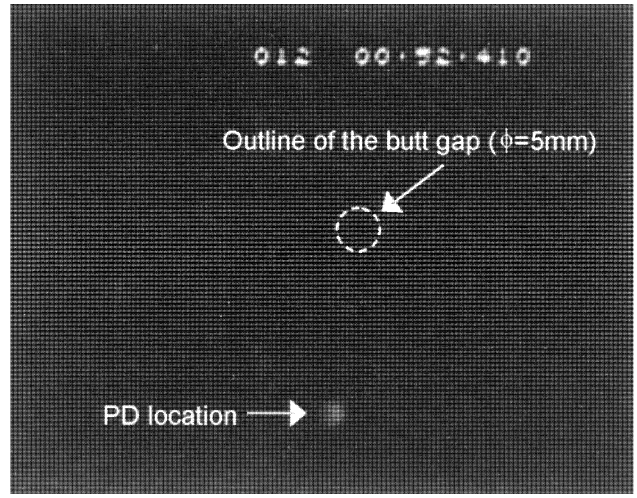

Figure 10. PD inception between laminated paper layers at $V_a = 30kV_{rms}$.

These results suggest that the equation (2) can be regarded as a universal expression for the volume effect on $PDIE_{50}$ for SSLV smaller than 50 mm^3 in a LN_2/PP laminated paper composite insulation system. The regression line in Figure 8 would be saturated at a certain level lower than 20 kV_{rms}/mm for the larger SSLV, as is in the case with the volume effect of conventional oil-filled transformers [11]. Further investigation will be necessary for the volume effect on $PDIE_{50}$ for the larger SSLV in a LN_2/PP laminated paper composite insulation system.

3.2 LIGHT EMISSION AT PD INCEPTION

In order to verify PD inception characteristics assumed above, we observed the PD light emission from between the PP laminated paper layers using experimental setup shown in Figure 9. Two PP laminated paper layers with a butt gap and one PET sheet were sandwiched between parallel plane electrodes. Grounded electrode was the transparent electrode made of glass and ITO film. The PD light emission was observed through the PET sheet, transparent electrode and the observation window in the cryostat (Figure 4), using an image intensifier and a high speed video camera.

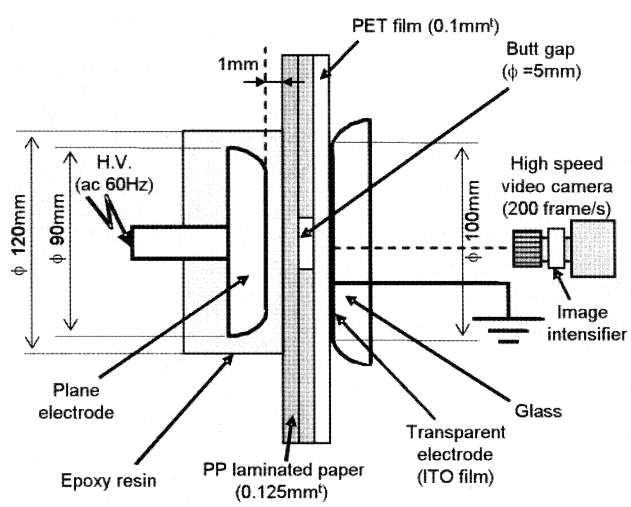

Figure 9. Experimental setup for optical observation of PD light emission.

Figures 10 and 11 show the light emission at PD inception observed outside the butt gap, i.e. between laminated paper layers, under the applied voltage of $V_a = 30\ kV_{rms}$ and $V_a = 24\ kV_{rms}$, respectively. Figure 11b shows the corresponding PD phase characteristics. The initial PD pulse signal was detected at around the peak of the applied voltage with the charge magnitude of about 100 pC. After the PD inception, PD pulses appeared regularly at around the zero-crossings of the applied voltage with the charge magnitudes smaller than that of initial PD. These results mean that PD inception between laminated paper layers generated thermal bubbles and induced the successive PDs in the bubbles. Figures 12a and 12b show the results of PD inception in a butt gap. PD light emission was intermittent with the corresponding single PD pulse, occurring near the peak of the positive half cycle.

The optical measurements of the PD light emission were repeated 16 times and revealed that initial PD was generated 12 times between the PP laminated paper layers and 4 times in butt gaps. These results support the concept of a SSLV parameter to describe the volume effect on $PDIE_{50}$ in such insulation system.

4 V-T CHARACTERISTICS AT PD INCEPTION

4.1 PD INCEPTION TIME

V-t characteristics obtained for different specimen configurations at the PD inception are summarized in Table 2. Weibull plots of PD inception times for specimen configurations A and F are shown in Figures 13a and 13b, respectively, where E_{ac} is the applied electric field, *a* is

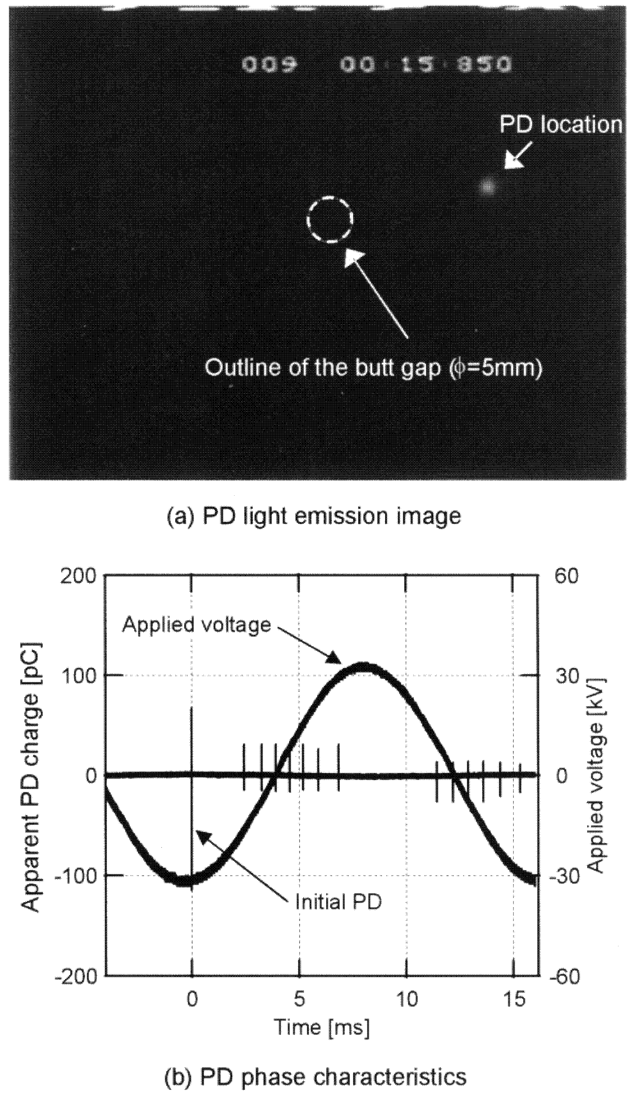

Figure 11. PD inception between laminated paper layers at $V_a = 24kV_{rms}$.

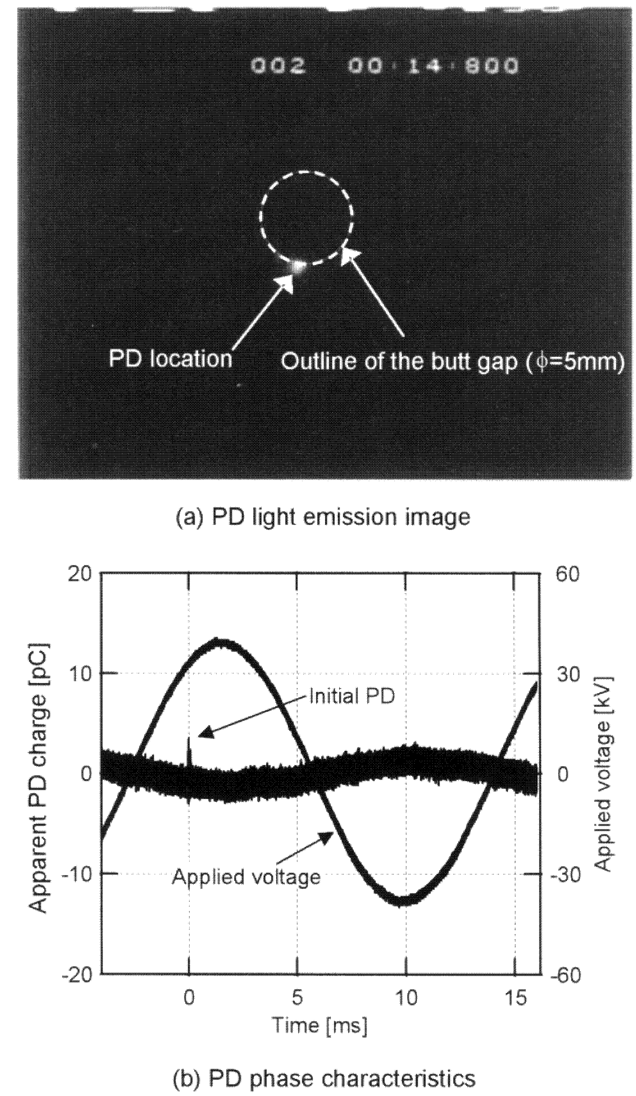

Figure 12. PD inception in a butt gap at $V_a = 28kV_{rms}$.

the shape parameter of the PD inception time distribution and t_{50} is the 50% percentile. The values of the shape parameter were lower than 1.0 for all experiments, which means that PD inception in LN_2/PP laminated paper composite insulation system is in the initial failure category.

Figure 14 shows V-t characteristics at PD inception for specimen configurations A, B and G. The lifetime indices n of V-t characteristics at PD inception were as high as 80-110, irrespective of the butt gap conditions. The n values for different specimen configurations and mechanical surface pressures on PP laminated paper are summarized in Table 2. The n values were higher than 80 for most butt gap configurations and surface pressures.

V-t characteristics at PD inception for two different hydrostatic pressures P in LN_2 are shown in Figure 15. PD inception stress at P = 0.15 MPa increased by about 30%, compared with that at P = 0.10 MPa. On the other hand, the n value was 88.2 at P = 0.10 MPa and 69.7 at P = 0.15 MPa, respectively; i.e. n value was almost constant or decreased slightly even under the pressurized condition.

4.2 COMPARISON OF N VALUES AT PD INCEPTION AND AT BREAKDOWN

The n values of V-t characteristics of the LN_2/PP laminated paper composite insulation taken at PD inception stresses differ from those at breakdown stresses. The n values for the V-t life curves were reported to be 15 to 89 [5–7], whereas at PD inception the n values are larger, 68 to 192. The difference in n values could be attributed to the difference in discharge mechanism.

As shown in Section 3, the PD inception could occur between laminated paper layers, in addition to discharges

Table 2. V-t equation for different butt gap conditions.

Specimen configuration		Surface pressure [N]	V-t equation
A	φ40, 3-layer 0 butt gap	15.2	$E=41.0\,t^{-1/111.5}$
B	φ40, 3-layer 1 butt gap	9.4	$E=37.4\,t^{-1/33.7}$
		15.2	$E=40.0\,t^{-1/88.2}$
		21.0	$E=40.9\,t^{-1/108.5}$
D	φ40, 3-layer 13 butt gap	4.9	$E=29.7\,t^{-1/68.4}$
E	φ40, 5-layer 0 butt gap	4.9	$E=35.3\,t^{-1/117.6}$
F	φ40, 5-layer 1 butt gap	9.7	$E=35.1\,t^{-1/117.6}$
G	φ40, 5 layer 3 butt gaps	4.9	$E=32.6\,t^{-1/192.2}$
		9.7	$E=34.2\,t^{-1/119.7}$
		15.5	$E=34.9\,t^{-1/86.8}$
H	φ70, 3-layer 1 butt gap	4.9	$E=24.1\,t^{-1/150.1}$

in butt gaps. PD light emission in Figure 11a was observed at PD inception under V_a = 24 kV_{rms}, which remained fixed at the same location even after the PD inception. When the applied voltage was raised to 30 kV_{rms}, another bright PD light emission shown in Figure 16 appeared in the entire space of the butt gap.

The above experimental results could be explained by the successive PD generation, i.e. PD inception between laminated paper layers would generate thermal bubbles with a dielectric strength lower than that of LN_2, and could induce successive PDs in those bubbles. PD light emission in the entire space of a butt gap also means the successive PD generation in gaseous N_2 bubbles. Breakdown would ultimately occur in such bubbles. The lower n value at breakdown can therefore be interpreted by intensification of PD development in thermal bubbles generated by preceding discharges.

5 CONCLUSIONS

IN this paper, we investigated the volume effect and the V-t characteristics both at PD inception in LN_2/PP laminated paper composite insulation system for HTS cables. The main results are summarized as follows:

1. PD inception stress (PDIE) cannot be evaluated only by the butt gap volume. Presence of weak points for PD inception in other than the butt gap areas has to be taken into account.

2. Statistically Stressed Liquid Volume (SSLV) parameter was introduced to evaluate the volume effect, with consideration of the discharge probability based on the electric field distribution not only in the butt gaps, but also in LN_2-filled thin layers between PP laminated sheets.

3. $PDIE_{50}$ decreased linearly in log-log scale with increasing SSLV for different butt gap numbers, PP laminated paper layers and electrode size.

	E_{ac} [kV_{rms}/mm]	$E_{ac}/PDIE_{50}$ [%]	t_{50} [s]	Confidence interval [s]	a
●	40.7	105	1.95	1.72–2.22	0.693
▲	39.7	102.5	34.1	27.9–41.7	0.914
■	38.8	100	397	285–553	0.425

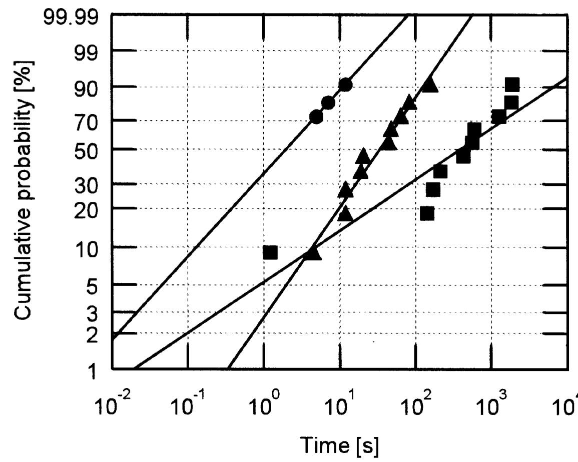

(a) Specimen configuration A (Fig.2) (3-layer without butt gap)

	E_{ac} [kV_{rms}/mm]	$E_{ac}/PDIE_{50}$ [%]	t_{50} [s]	Confidence interval [s]	a
●	35.9	105	0.07	0.05–0.10	0.246
▲	34.9	102.5	5.59	4.66–6.69	0.416
■	34.1	100	10.5	7.6–14.5	0.233
◆	33.3	97.5	502	173–1454	0.192

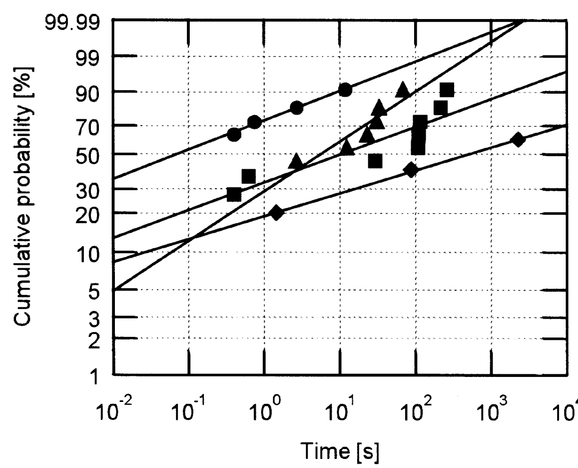

(b) Specimen configuration F (Fig.2) (5-layer with one butt gap)

Figure 13. Weibull plots of PD inception times.

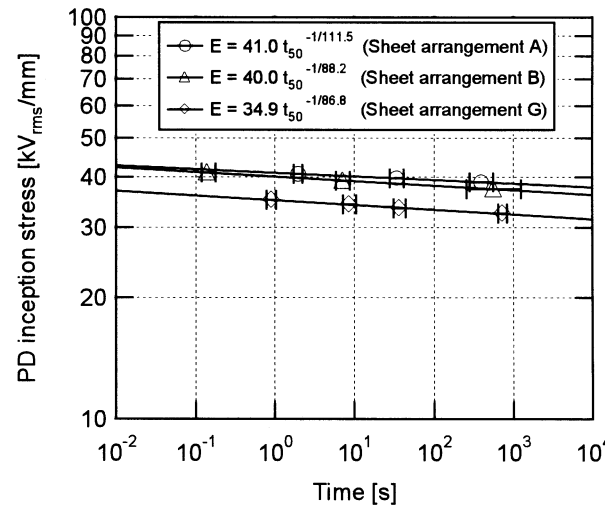

Figure 14. V-t characteristics at PD inception for different butt gap conditions specimens A, B and G.

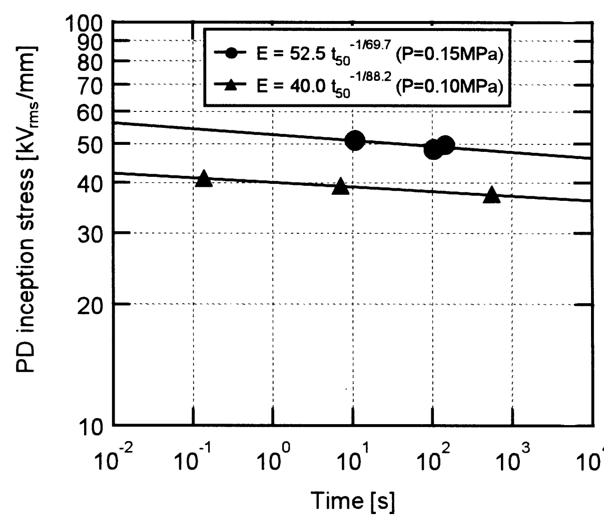

Figure 15. V-t characteristics at PD inception for different hydrostatic pressures in LN_2 specimen B.

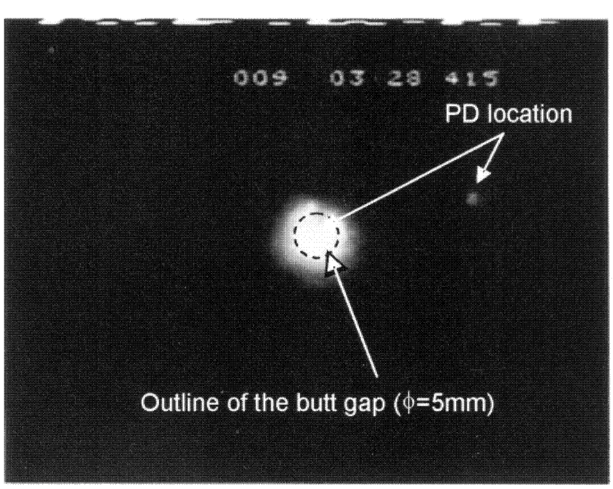

Figure 16. PD light emission image at $V_a = 30kV_{rms}$ after PD inception at $V_a = 24kV_{rms}$.

4. Light emission due to PD inception was detected not only inside the butt gaps, but also outside and this supports the concept of the SSLV and the volume effect on $PDIE_{50}$ in PP laminated paper insulation for HTS cables.

5. Lifetime indices n of V-t characteristics at PD inception were as high as 80-110, irrespective of butt gap conditions. The n value decreased slightly under pressurized LN_2 condition.

6. The lower n values at breakdown were interpreted by the intensified PD development in thermal bubbles generated by partial discharges.

ACKNOWLEDGMENT

This work has been carried out as a part of Super-ACE (the research and development of fundamental technologies for superconducting ac power equipment) project of METI (the Ministry of Economy, Trade and Industry), as a contract research from NEDO (the New Energy and Industrial Technology Development Organization).

REFERENCES

[1] T. Masuda, T. Kato, H. Yumura, M. Watanabe, Y. Ashibe, K. Ohkura, C. Suzawa, M. Hirose, S. Isojima, K. Matsuo, S. Honjo, T. Mimura, T. Kuramochi, Y. Takahashi, H. Suzuki and T. Okamoto, "Verification Tests of a 66kV HTSC Cable System for Practical Use (first cooling tests)", Physica C, Vol. 378–381, No. 2, pp. 1174–1180, 2002.

[2] D. Willén, F. Hansen, M. Däumling, C. N. Rasmussen, J. Østergaard, C. Traeholt, E. Veje, O. Tønnesen, K. H. Jensen, S. K. Olsen, C. Rasmussen, E. Hansen, O. Schuppach, T. Visler, S. Kvorning, J. Schuzster, J. Mortensen, J. Christiansen and S. D. Mikkelsen, "First Operation Experiences from a 30 kV, 104MVA HTS Power Cable Installed in a Utility Substation", Physica C, Vol. 372–376, No. 3, pp. 1571–1579, 2002.

[3] P. Corsaro, M. Bechis, P. Caracino, W. Castiglioni, G. Cavalleri, G. Coletta, G. Colombo, P. Ladiè, A. Mansoldo, R. Mele, S. Montagner, C. Moro, M. Nassi, S. Spreafico, N. Kelley and C. Wakefield, "Manufacturing and Commissioning of 24 kV Superconducting Cable in Detroit", Physica C, Vol. 378–381, No. 2, pp. 1168–1173, 2002.

[4] P. Caracino, M. Lakner, H. Okubo, O. Tønnesen and B. Wacker, "Superconducting and Insulating Materials for HTS Power Applications", CIGRE 15–405, 2002.

[5] S. Mukoyama, M. Yagi, S. Tanaka, K. Matsuo, S. Honjo, T. Mimura, T. Aiba and Y. Takahashi, "Development of Important Elementary Technologies for a 66kV-Class Three-phase HTS Power Cable", Physica C, Vol. 378–381, No. 2, pp. 1181–1184, 2002.

[6] G. M. Hathaway, A. E. Davies and S. G. Swingler, "Dielectric Considerations for a Superconducting Cable Termination", ISH, Vol. 4, No. 467, pp. 84–87, 1999.

[7] A. Bulinski, J. Densley and T. S. Sudarshan, "The Ageing of Electrical Insulation at Cryogenic Temperature", IEEE Trans. Electr. Insul., Vol. 15, No. 2, pp. 83–88, 1980.

[8] M. Hazeyama, T. Kobayashi, N. Hayakawa, S. Honjo, T. Masuda and H. Okubo, "Partial Discharge Inception Characteristics under Butt Gap Condition in Liquid Nitrogen/PPLP® Composite Insulation System for High Temperature Superconducting Cable", IEEE Trans. Dielectr. Electr. Insul., Vol. 9, pp. 939–944, 2002.

[9] H. Okubo, M. Hazeyama, N. Hayakawa, S. Honjo and T. Masuda, "V-t Characteristics at Partial Discharge Inception in Liquid Nitrogen/PPLP® Composite Insulation System for HTS Cable", IEEE Trans. Dielectr. Electr. Insul., Vol. 9, pp. 945–951, 2002.

[10] H. Goshima, N. Hayakawa, M. Hikita, H. Okubo and K. Uchida, "Weibull Statistical Analysis of Area and Volume Effects on Breakdown Strength in Liquid Nitrogen", IEEE Trans. Dielectr. Electr. Insul., Vol. 2, pp. 385–393, 1995.

[11] Y. Kawaguchi, H. Murata and M. Ikeda, "Breakdown of Transformer Oil", IEEE Trans. Power Appar. Systems, Vol. 91, pp. 623–629, 1972.

Naoki Hayakawa (M'90) was born on 9 September 1962. He received the Ph.D. degree in 1991 in electrical engineering from Nagoya University. Since 1990, he has been at Nagoya University and presently is an Associate Professor of Nagoya University at the Department of Electrical Engineering and Computer Science. From 2001 to 2002, he was a guest scientist at the Forschungszentrum Karlsruhe/Germany. He is also a member of IEE of Japan.

Tsuyoshi Kobayashi was born on 21 November 1979. He received the B.S. degree in 2004 in energy, engineering and science from Nagoya University. In 2004 he joined Chuba Electric Power Co. Ltd., Japan.

Moriyuki Hazeyama was born on 9 February 1978. He received the Ph.D. degree in 2003 in electrical engineering from Nagoya University. He joined Mitsubishi Electric Corporation, Japan in 2003. He is also a member of IEE of Japan.

Toshihiro Takahashi (M'02) was born on 25 April 1973. He received the Ph.D. degree in 2001 in electrical engineering from Nagoya University. He joined Yokosuka Research Laboratory of the Central Research Institute of Electric Power Industry (CRIEPI), Kanagawa, Japan in 2001 and is now the research scientist of Electric Power Engineering Research Laboratory, CRIEPI. He has been engaged in the study of SF_6 gas, solid and cryogenic insulations. He was a guest scientist at IREQ, Canada, in 2002. He is also a member of IEE of Japan.

Kenji Yasuda was born on 15 October 1955. He received the B.S. degree in 1978 in electrical engineering from Gifu University. He joined Chubu Electric Power Co., Ltd., Japan in 1978 and had been engaged in research on transmission line constructions and maintenance of power equipment. He was temporally transferred to the Institute of Applied Energy from 1989 to 1991. Since 2002, he has been temporally transferred to the Engineering Research Association for Superconductive Generation Equipment and Materials, Japan, and now is a project manager of R & D of fundamental technologies for superconducting AC power equipment.

Hitoshi Okubo (M'81) was born on 29 October 1948. He received the Ph.D. degree in 1984 in electrical engineering from Nagoya University. He joined Toshiba Corporation, Japan in 1973 and was a manager of high voltage laboratory of Toshiba. From 1976 to 1978, he was at the RWTH Aachen, Germany and the TU Munich, Germany. In 1989, he became an Associate Professor of Nagoya University at the Department of Electrical Engineering and presently he is a Professor of Nagoya University at the EcoTopia Science Institute. He is a member of IEE of Japan, VDE and CIGRE.

